



ELSEVIER

Journal of Alloys and Compounds 311 (2000) 1–10

Journal of
ALLOYS
AND COMPOUNDS

www.elsevier.com/locate/jallcom

Rare earth magnetism in high-temperature and borocarbide superconductors

P. Allenspach*, U. Gasser

Laboratory for Neutron Scattering, ETH Zurich and PSI Villigen, 5232 Villigen PSI, Switzerland

Abstract

High-temperature superconductors possess – besides their superconductivity – other fascinating features such as a rich magnetic phase diagram. While it is normally believed that superconductivity and rare-earth magnetism is decoupled in these systems a closer investigation clearly proves that both effects in a very similar manner depend on the doping of charge carriers. An inhomogeneous charge distribution results in inhomogeneous superconductivity and a loss of long-range magnetic order. Magnetic borocarbides are ideal model systems for an investigation into the interaction of superconductivity and (collective) magnetism due to their similar values for the critical temperature of superconductivity and the magnetic ordering temperature. Both lie typically below 15 K and are hence in a comfortable temperature regime for measurements. We will present for both classes of the above substances an analysis based on a wide variety of different measurements (susceptibility, specific heat, neutron diffraction and spectroscopy). This analysis provides an almost universal, phenomenological picture of their magnetic properties. © 2000 Elsevier Science S.A. All rights reserved.

Keywords: Superconductors; Borocarbides; Magnetic interaction; Neutron scattering; Specific heat

1. Introduction

High-temperature superconductors of type $\text{RBa}_2\text{Cu}_3\text{O}_x$ (R:Y and most rare earths; $6 \leq x \leq 7$; in the following called R123x) are probably the most intensely investigated systems. Of course this is mainly due to the fact that they are superconducting at high temperatures. But in the process of investigation, a full wealth of fascinating features in a very restricted range of (hole) doping – by varying the oxygen content – was discovered. This includes a metal–insulator transition, a pseudo-gap, possible charge ordering, electronic phase separation, long-range magnetic order of Cu and magnetic order of rare earth ions. The rare earth magnetic order (T_N typically around 1 K) turned out to be very much dependant on doping, but not via the direct influence of the variation of the oxygen content, but via the hole carriers induced by the introduction of oxygen [1]. The resulting complicated magnetic behavior will be described as a competition of different interactions.

$\text{RB}_2\text{Ni}_2\text{C}$ (R:Y and most rare earths; in the following called RBNC) are borocarbide superconductors with critical temperatures T_c between 0 and 25 K and magnetic ordering temperatures T_m between 0 and 15 K, depending on the rare earth ion [2]. These are intermetallic systems

with dominating magnetic interactions of the RKKY-type and almost classical BCS-superconductivity. Long-range magnetic ordering (with coherent magnetic excitations) is compatible with superconductivity, while magnetic phase transitions and hence incoherent magnetic fluctuations seem to be detrimental for superconductivity.

In the first part of this paper, we will concentrate on the possible magnetic interactions in rare earth containing compounds. As it turns out not all of the possible interactions are really of importance for the compounds in question. But as we will demonstrate further on, only the competition of some of the remaining interactions lead to the observed magnetic behavior in the high-temperature superconductors, while for the borocarbides one interaction is clearly dominant. The interest in borocarbides is mainly focused on the interaction of superconductivity and long-range magnetic order since both effects are of similar size. Unfortunately, experimental data suited for the elaboration of a theory of this coexistence are still sparse.

2. Different magnetic interactions

Since the $4f$ electrons in rare earth ions (responsible for the magnetism) lie well within the outer $5s$, $5d$ and $6s$ shells their spatial extent is very limited and a direct overlap with the $4f$ shell of neighboring rare earth ions is only realized in systems with very closed packed rare earth

*Corresponding author. Tel.: +41-56-310-2527; fax: +41-56-310-2939.

E-mail address: peter.allenspach@psi.ch (P. Allenspach).

ions. In the compound families discussed in this paper, the distance between the two rare earth ions is relatively large (for R123x and for RBNC), hence this direct exchange can be neglected in the further study. All measurements point to very localized moments in both of these compound families (with a few exceptions: Pr123x and YbBNC) which excludes itinerant magnetism from the list. In the following we will discuss the remaining magnetic interactions which may play an important role in the magnetic properties of R123x and RBNC.

2.1. Hyperfine interaction

The hyperfine interaction couples the electronic magnetism of the $4f$ electrons to that of the nuclear moment. Almost all of the ions in R123x and RBNC possess a non-vanishing nuclear moment and hyperfine interaction is always present. The strength of the interaction is normally very weak and only important at temperatures well below 1 K. For R123x and RBNC no sizeable hyperfine effects were observed except for Ho123x ($T_m=39$ mK) [3].

2.2. Dipolar interaction

Magnetic moments are interacting with each other via their dipolar magnetic field. The interaction is long range in nature as can be seen from its Hamiltonian:

$$\hat{H}_{\text{dip}} = \sum_{i \neq j} \left[\frac{\vec{\mu}_i \cdot \vec{\mu}_j}{r_{ij}^3} - 3 \frac{(\vec{\mu}_i \cdot \vec{r}_{ij})(\vec{\mu}_j \cdot \vec{r}_{ij})}{r_{ij}^5} \right]. \quad (1)$$

$\vec{\mu}_i$ denotes the magnetic moment at site i and \vec{r}_{ij} the direction vector from site i to site j . If one assumes the moments to be parallel or antiparallel (Ising spins) to each other and the size of the moment not to be site dependent the Hamiltonian [Eq. (2)] simplifies to:

$$\hat{H}_{\text{dip}} = \sum_{i \neq j} \left[\pm \frac{\mu^2}{r_{ij}^3} (1 - 3 \cos \theta_{ij}) \right], \quad (2)$$

where θ_{ij} is the angle between \vec{r}_{ij} and the (fixed) moment direction. The unit of dipolar energy (for lengths in Å and moments in μ_{Bohr}) is $\mu_B^2/\text{Å}^3 = 5.368 \cdot 10^{-2}$ meV = 0.623 K. Hence, the dipolar coupling strength for a typical rare earth distance of 3.8 Å and a moment of 7 μ_{Bohr} perpendicular to the distance vector (as in Dy1237) is 0.56 K, and T_N would then be about 0.64 K. Obviously, a large magnetic moment is needed to obtain ordering temperatures of the order of 1 K, since the coupling strength is proportional to the square of the moment.

2.3. Superexchange

In contrast to the dipolar interaction the superexchange interaction is of very short range (essentially next neigh-

bors). Therefore, the hamiltonian can be written as a Heisenberg spin Hamiltonian:

$$\hat{H} = -2 \sum_{\langle i,j \rangle} J_{ij} (S_i \cdot S_j), \quad (3)$$

where the summation runs over all rare earth pairs $\langle i,j \rangle$ and S_i denote the spin operators, J_{ij} is a tensor which magnetically couples the pair $\langle i,j \rangle$. In the majority of cases for an explanation of the experimental data, only the diagonal terms J^{xx} , J^{yy} and J^{zz} are taken into account. If these three values are identical a pure Heisenberg model is realized. For $|J^{zz}| > 0$ and $J^{xx} = J^{yy} = 0$ we are left with a Ising model and for $J^{zz} = 0$ and $|J^{xx}| = |J^{yy}| > 0$ with a XY-model, respectively. Positive signs denote ferromagnetic and negative signs antiferromagnetic coupling. The interaction is mediated via the polarization of ligand electrons by the $4f$ -electrons of the rare earth ion. These polarized ligand electrons in return polarize the $4f$ -electrons of the next rare earth ion. These bridging ligand ions are as such non-magnetic. Superexchange is observed in semiconducting materials and results in ordering temperatures of the order of 1 K (in rare earth compounds). Hence, for systems with a large magnetic moment a competition between dipolar and superexchange interaction may be observed.

2.4. Indirect exchange (RKKY interaction)

The RKKY interaction (after Ruderman, Kittel, Kasuya and Yosida) is mediated via a polarization of the charge carriers by the $4f$ -electrons of the rare earth ions, and hence very similar as the superexchange interaction. But for the RKKY interaction – in contrast to superexchange – obviously some charge carriers have to be present. This interaction is therefore dominant in rare earth metals and intermetallics and leads to ordering temperatures of up to room temperature. As for superexchange, the RKKY Hamiltonian can be written in the Heisenberg spin Hamiltonian form of Eq. (3). But instead of a fixed value for the coupling of a pair, J_{ij} , the coupling is distance dependent and can (according to Jensen and Mackintosh [4]) be written in its simplest form as

$$J(R) = 12\pi\nu |j_0|^2 \bar{N}(E_F) \frac{\sin(2k_F R) - 2k_F R \cos(2k_F R)}{(2k_F R)^4}, \quad (4)$$

where ν is the number of conduction electrons per ion, $|j_0|$ is the fixed effective exchange integral, $\bar{N}(E_F)$ is the excess number of spin-up electrons due to the splitting of the spin-up and spin-down band and k_F the Fermi wave vector. The strength of the coupling is oscillating and for large distances goes as R^{-3} . Hence, the RKKY interaction is long-range in nature and the sum over all pairs in Eq. (3) has to be taken. An example for this oscillating behavior is shown for $k_F = 0.55 \text{ Å}^{-1}$ in Fig. 1.

For both, superexchange and RKKY interaction, the Hamiltonian in Eq. (3) neglects – since it is a pure spin

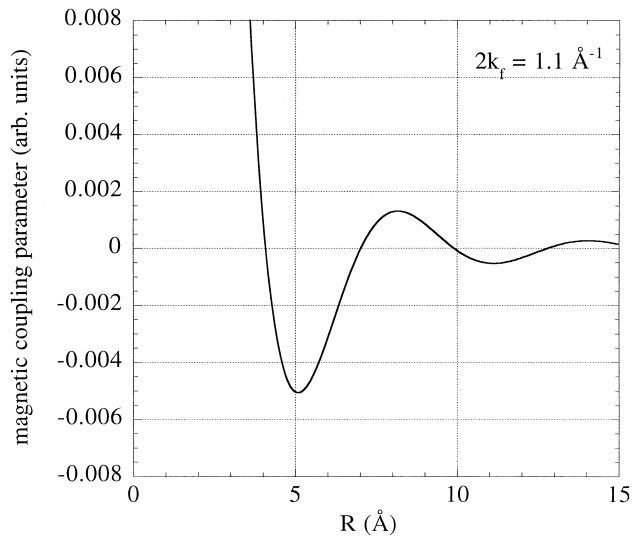


Fig. 1. Behavior of the RKKY coupling as a function of distance.

hamiltonian – the influence of the actual total angular momentum \mathbf{J} and the magnetic behavior would be identical for all rare earths independent of their difference in \mathbf{J} . In order to compensate for that, one has to multiply the right side of the equation by the de Gennes factor $(g_j - 1)^2 \cdot J(J + 1)$.

3. Magnetic interactions in high-temperature superconductors

3.1. Fully oxidized R1237

The magnetic properties of high temperature superconductors of the type R123x have been studied extensively in the past [5,6]. We will concentrate here on the systems with ordering temperatures above 0.5 K and which contain Kramers ions (i.e. Nd [$T_N = 0.53$ K], Sm [$T_N = 0.61$ K], Dy [$T_N = 0.91$ K] and Er [$T_N = 0.60$ K]). The onset of long-range magnetic ordering can clearly be seen in the sharp anomaly in the specific heat (Fig. 2). It was shown in the past that the antiferromagnetic ordering temperatures follow roughly the de Gennes scaling [7] and that the anomalies can very well be modeled by an anisotropic two-dimensional (2D) spin-1/2 Ising model [8]. A good de Gennes scaling indicates exchange interaction (be it superexchange or RKKY); dipolar interaction would result in ordering temperatures proportional to the square of the ordered magnetic moment. Nevertheless, as mentioned above, dipolar interaction cannot be ruled out for ordering temperatures below 1 K. Since these compounds are layered systems, a good agreement with a 2D-model can be expected (here the agreement is actually excellent). What is more surprising is the fact that a Ising model is sufficient to explain these anomalies. The single-ion anisotropy of Dy in Dy123 – deduced from crystalline electric

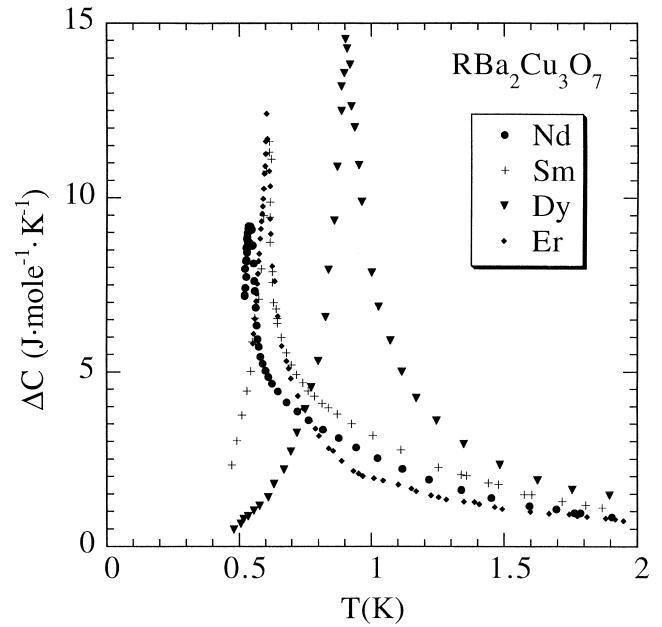


Fig. 2. Magnetic specific heat of NdBa₂Cu₃O₇ [7], SmBa₂Cu₃O₇, DyBa₂Cu₃O₇ and ErBa₂Cu₃O₇ [8].

field (CEF) measurements – makes it almost a Ising system [9], but Nd [10] is almost isotropic and Sm [11] and Er [12] planar. (For CEF effects in these compounds see also Ref. [13].) The other surprising thing is the large in-plane anisotropy of the coupling constants into the two plane directions ($J_1/J_2 = 50, 11, 4$ and 5 for Nd, Sm, Dy and Er, respectively). All of these four rare earth ions in R123 exhibit a well isolated CEF doublet ground state, hence the application of an effective spin-1/2 model can be justified. The low ordering temperatures and the fact that the dipolar model and the 2D-Ising model belong to the same universality class makes a further investigation of the dipolar interaction in these compounds necessary. We follow here the Monte-Carlo approach exemplified by MacIsaac et al. [14] who calculated the dipolar interaction and subsequently the exchange interaction of a planar patch of magnetic moments. For the value and the direction of the moment we took for our calculations the values obtained from neutron diffraction (together with neutron structural data) and the experimental ordering temperatures from the specific heat measurements (Table 1). The calculated ordering temperature for Nd123 and Sm123 is – due to the small moments – two orders of magnitude smaller than observed and the dipolar interaction is of no importance for these two compounds. This is in contrast to the calculated ordering temperatures for Er123 and Dy123 which are equal or almost equal to the experimental values. In a second step the ordering temperature as well as the shape of the specific heat anomaly was modeled with a combination of a dipolar and an exchange (nearest-neighbor) coupling. The raw values (J_{calc}) and the values corrected with the de Gennes factor (J_{corr}) are given in

Table 1

Measured in-plane lattice constants and size and direction of the magnetic moments as well as the ordering temperatures used for the calculations (the values differ hardly from author to author)^a

Rare earth	a (Å)	b (Å)	$ \mu $ (μ_B)	μ -direction	T_N^{ex} (K)	T_N^{calc} (K)	J_{calc} (μeV)	J_{corr} (μeV)
Nd123	3.86	3.91	1.14	c	0.52	<0.02	−59/−3.5	−323.0/−19.2
Sm123	3.84	3.90	0.34	a	0.61	<0.02	−60/−5.4	−83.0/−7.5
Dy12	3.82	3.89	6.8	c	0.91	0.64	−8/−8.0	−2.8/−2.8
Er123	3.81	3.88	4.9	b	0.60	0.61	−12/−12.0	−18.0/−18.0

^a The calculated values for the ordering temperature (with dipolar interactions only) as well as the magnetic exchange constants (dipolar+exchange interaction calculations) are given. J_{corr} lists the exchange constants corrected with the modified de Gennes factor (see text).

Table 1. The choice of antiferromagnetic exchange constants is the result of observations of the magnetic ordering in systems with small influences from the dipolar interaction and the consideration of consistency (same sign for the exchange interaction for all the rare earths): For Nd where the dipolar interaction is weak (hence the magnetic ordering is controlled by the exchange interaction) antiferromagnetic ordering within the plane has been observed by neutron diffraction [15]. Obviously, the magnetic exchange coupling is largest for the lighter but bigger rare earth ions Nd and Sm. This trend is more pronounced by going to the even larger Pr in Pr123 where the magnetic ordering temperature due to exchange is almost 20 K [16]. This increased hybridization also leads eventually, for Pr123, to a suppression of superconductivity.

3.2. Oxygen dependence

Oxygen reduction in R123x leads to a decrease in T_c which is dependent on the rare earth [17]. For light rare earth ions the decrease is rather rapid, while for the heavier ones the superconducting regime spans down to very low oxygen contents. This larger range of superconductivity is mainly due to the occurrence of the plateau structure of $T_c(x)$ observed for the heavier rare earths. At a certain oxygen content (about 6.6 for Nd and 6.35 for Er) a transition from metallic to semiconducting behavior is observed. The reduction of the oxygen content causes a reduction of the mobile charge carriers (holes) in the CuO_2 -planes which is well documented by transport measurements. Such a variation of the carrier density is not expected to affect the dipolar interaction directly, but it may be influenced via a oxygen dependence of the lattice constants or the CEF. The former effect modifies the dipolar energy proportional to r^{-3} , while the latter may alter the size of the moment. (With neutron diffraction and CEF spectroscopy it was shown that the moment in oxygen reduced samples are slightly smaller than in fully oxidized samples). These modifications in the dipolar interaction can be calculated directly and hence will not yield unexpected results. RKKY interaction – the indirect exchange via the conduction electrons – will vitally depend on the density of charge carriers. Since the fully oxidized samples show a metallic and the reduced a semiconducting behavior the RKKY interaction is expected to weaken

drastically by going from oxygen content $x=7$ (metallic fully oxidized RKKY strong) to $x=6$ (semiconducting reduced RKKY weak). A semiconducting or insulating matrix is ideal for the superexchange interaction, therefore, superexchange is expected to be dominant in the reduced samples. The expectation for intermediate oxygen (intermediate hole carrier) concentration is a superexchange influenced by a sea of free carriers and hence a competition between superexchange and RKKY interaction as described by Gonçalves da Silva and Falicov [18]. Carrier density variations in the sample will then obviously have a strong influence on the magnetic ordering if both exchange interactions start to be similar in size.

Indeed, a very strong oxygen dependence of the magnetic ordering was found for these compounds (Fig. 3). All order in a long range manner at high oxygen contents (as seen before) and almost long range at very low oxygen contents (this was also confirmed by neutron diffraction [5]). But in the intermediate oxygen regime (on the metal side of the metal–insulator transition) the magnetic ordering turns out to be short range (broad anomalies in the specific heat). With the aim to obtain a consistent behavior for the oxygen dependence of the exchange parameters for the four compounds we used our model (dipolar and nearest neighbor exchange interaction) to reproduce the specific heat anomalies in the metallic (superconducting) regime. The details of the analysis can be found in Ref. [6]. The resulting calculated specific heat anomalies are shown in Fig. 4 together with the coupling constants. The anomalies in the calculation are – due to the limited cluster size used – broader than the observed ones, but qualitatively they are in good agreement with the measurements shown in Fig. 3. A ferromagnetic coupling (positive sign) in one direction of the plane is necessary but not sufficient to explain the experimental data. A random (dynamic) distribution of the two couplings J_1 and J_2 into the two different planar directions is also needed. Complicated effects on the magnetic ordering including ferromagnetic coupling are predicted by varying the charge carrier density in the range where superexchange and RKKY interaction are comparable [18]. But these would always result in long-range magnetic order. The random distribution has most likely its origin in the strong charge carrier disorder observed in neutron spectroscopy for the intermediate oxygen content [19]. This disorder may affect

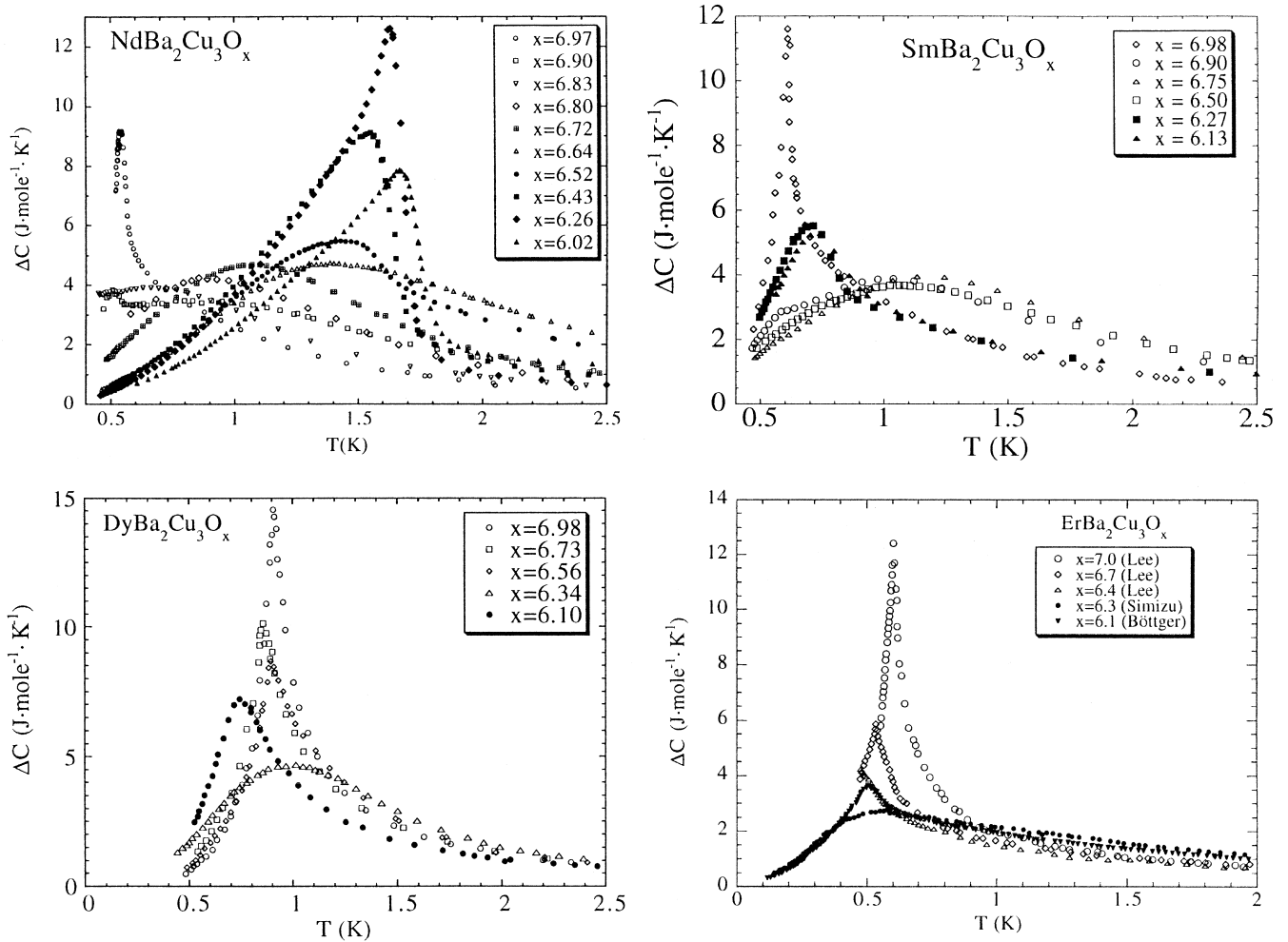


Fig. 3. Oxygen dependence of the magnetic ordering of $\text{NdBa}_2\text{Cu}_3\text{O}_x$, $\text{SmBa}_2\text{Cu}_3\text{O}_x$, $\text{DyBa}_2\text{Cu}_3\text{O}_x$ and $\text{ErBa}_2\text{Cu}_3\text{O}_x$ [6]. The open symbols denote superconducting and the filled symbols non-superconducting samples.

both superexchange as well as RKKY interaction, but up to now neither experimental data nor theory are available for a microscopic explanation of the effect of disorder on the magnetic coupling. As a final remark we would like to note here that the very same charge carriers which are responsible for this odd behavior of the magnetic order promote also superconductivity.

4. Magnetic interactions in borocarbide superconductors

Although the chemical structure of the borocarbides consists of (R,C)-layers alternating with (Ni_2B_2) -layers, their electronic structure is clearly three-dimensional [20–22]. Only a small anisotropy has been found in $\text{YNi}_2\text{B}_2\text{C}$. The temperatures of magnetic ordering in the borocarbides lie between 1.5 and 15 K, which is too high for the dipole interaction to play a significant role. Furthermore, the accurate scaling of T_m with the de Gennes factor is evidence for the RKKY and against the dipole interaction.

This is in contrast to the magnetic superconductors RRh_4B_4 ($\text{R}=\text{Nd, Sm, Er}$ and Tm) and RMO_6S_8 ($\text{R}=\text{Nd, Gd, Tb, Dy, Ho}$ and Er) as well as RMO_6Se_8 ($\text{R}=\text{Gd, Tb, Ho}$ and Er) that have been discovered in the late 1970s. There, the temperatures of magnetic ordering are about one order of magnitude smaller than in the borocarbides (typically 1 K). For the coexistence of superconductivity with magnetic order, the dipole interaction is an advantage since the conduction electrons are only involved in the formation of the superconducting state and do not play an active role for the magnetic exchange. This is an advantage for the coexistence of the two phenomena because the electrons that are bound in Cooper pairs in the superconducting state cannot be polarized and therefore do not contribute to exchange interactions. On the other hand this implies that the coexistence of magnetic order with superconductivity is even more surprising in the borocarbides: The conduction electrons play a key role for both superconductivity and magnetic order. From Eq. (4) it becomes clear that the RKKY interaction will lead to magnetic orders with a large wavelength. As it does not have a direct

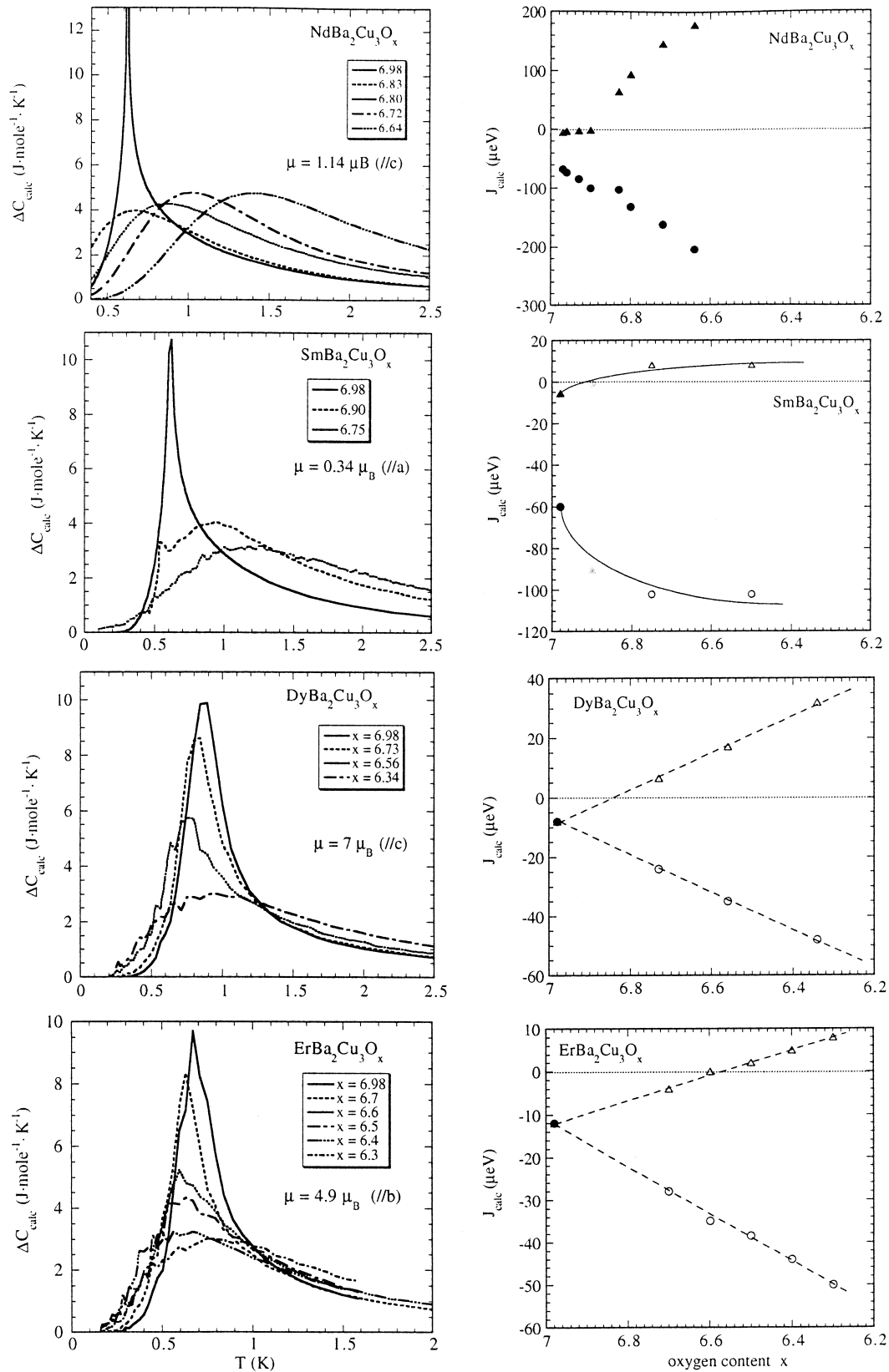


Fig. 4. Calculated oxygen dependence for the superconducting species of Nd123x, Sm123x, Dy123x and Er123x (left) and oxygen dependence of the magnetic exchange constants (right) used for the calculation of the specific heat anomalies. The open symbols indicate parameters with random distribution (see text). (For Nd123x a slightly different approach was used [29].)

connection with the chemical structure but rather depends on the details of the electronic structure, incommensurate magnetic structures are typical for the RKKY interaction. This is what has been found in some of the RNi_2B_2C compounds ($R = Gd, Er$ and Tm ; see Fig. 5). Nevertheless, the majority of the borocarbide compounds shows magnetic structures that are commensurate with the chemical lattice [23]. This emphasizes the importance of the second major ingredient for the understanding of their magnetism: the single ion anisotropy. For the rare earth ions the directions of the hard and easy axes are determined by the crystalline electric field [24,25]. In contrast to the RKKY interaction, the existence of easy directions favors a parallel, commensurate alignment of the magnetic moments ($R = Pr, Nd, Dy$ and Ho). The big variety of magnetic structures (Fig. 5) in the borocarbides is the product of the competition of the long-range RKKY interaction with the single-ion anisotropy due to the CEF. In some RNi_2B_2C compounds the equilibrium between RKKY exchange and single ion anisotropy is very delicate.

4.1. $HoNi_2B_2C$

A magnetic phase transition occurs just below $T_c \sim 8$ K. Between 8 and 5 K Bragg peaks belonging to an antiferromagnetic and an incommensurate helical structure are observed at the same time. The relative intensities of the Bragg peaks of the commensurate and the incommensurate structure vary from sample to sample, and the two magnetic orders are therefore believed to belong to different regions of the samples [23]. This stresses the delicate dependence of the realized magnetic order on the details of sample composition and quality. A second magnetic phase transition occurs at $T_N \sim 5$ K, where the helix phase disappears and only the commensurate antiferromagnetic order survives at lower temperatures. Measurements of the temperature dependence of the upper critical field H_{c2} of superconductivity and the magnetic susceptibility show that this phase transition is linked with a strong suppression of superconductivity. In some samples even reentrance of superconductivity has been observed. Another

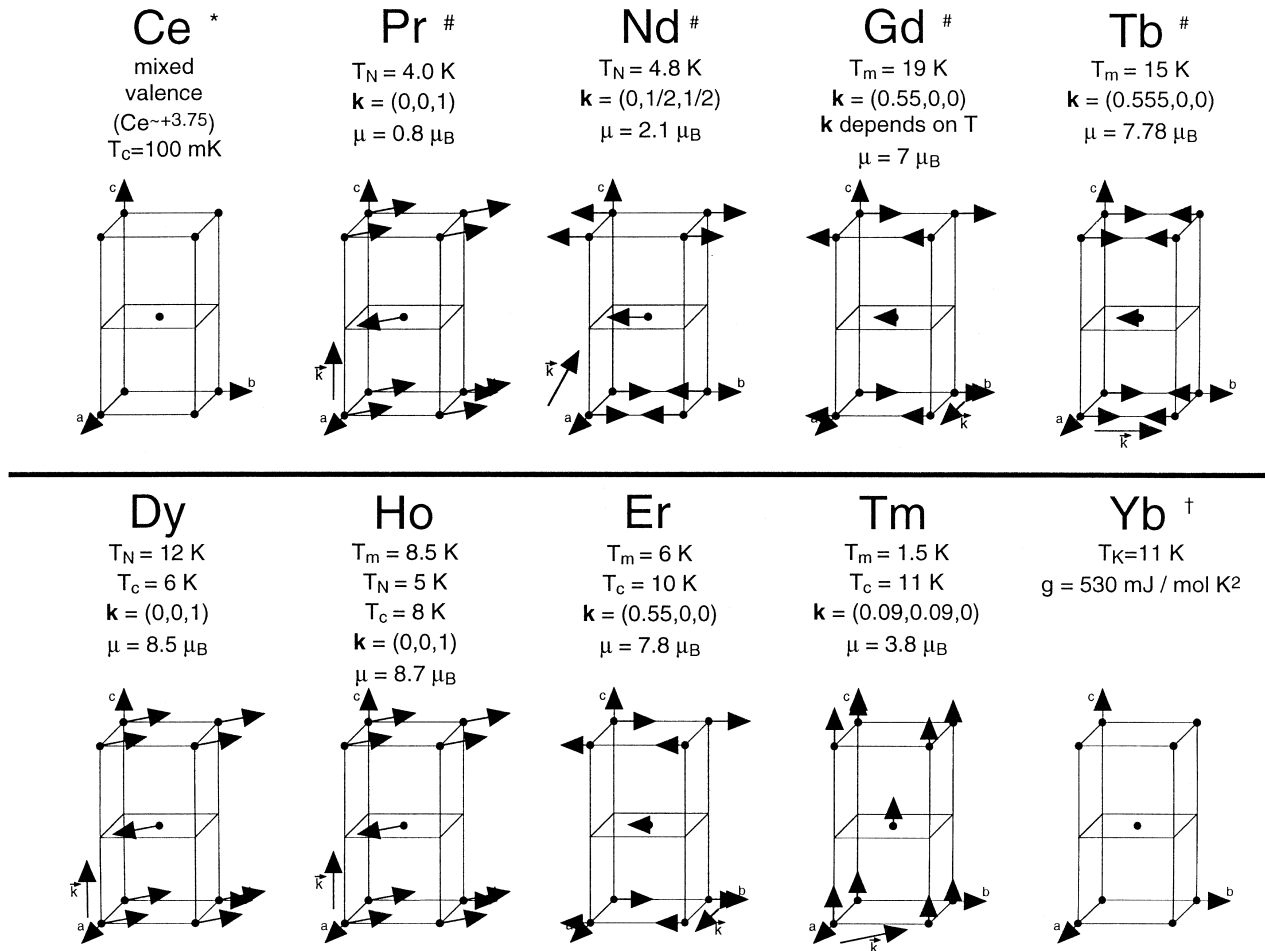


Fig. 5. A overview of the magnetic ordering in RNi_2B_2C . (*, mixed valent; #, non-superconducting; †, heavy fermion, non-superconducting; the rest are superconducting systems.)

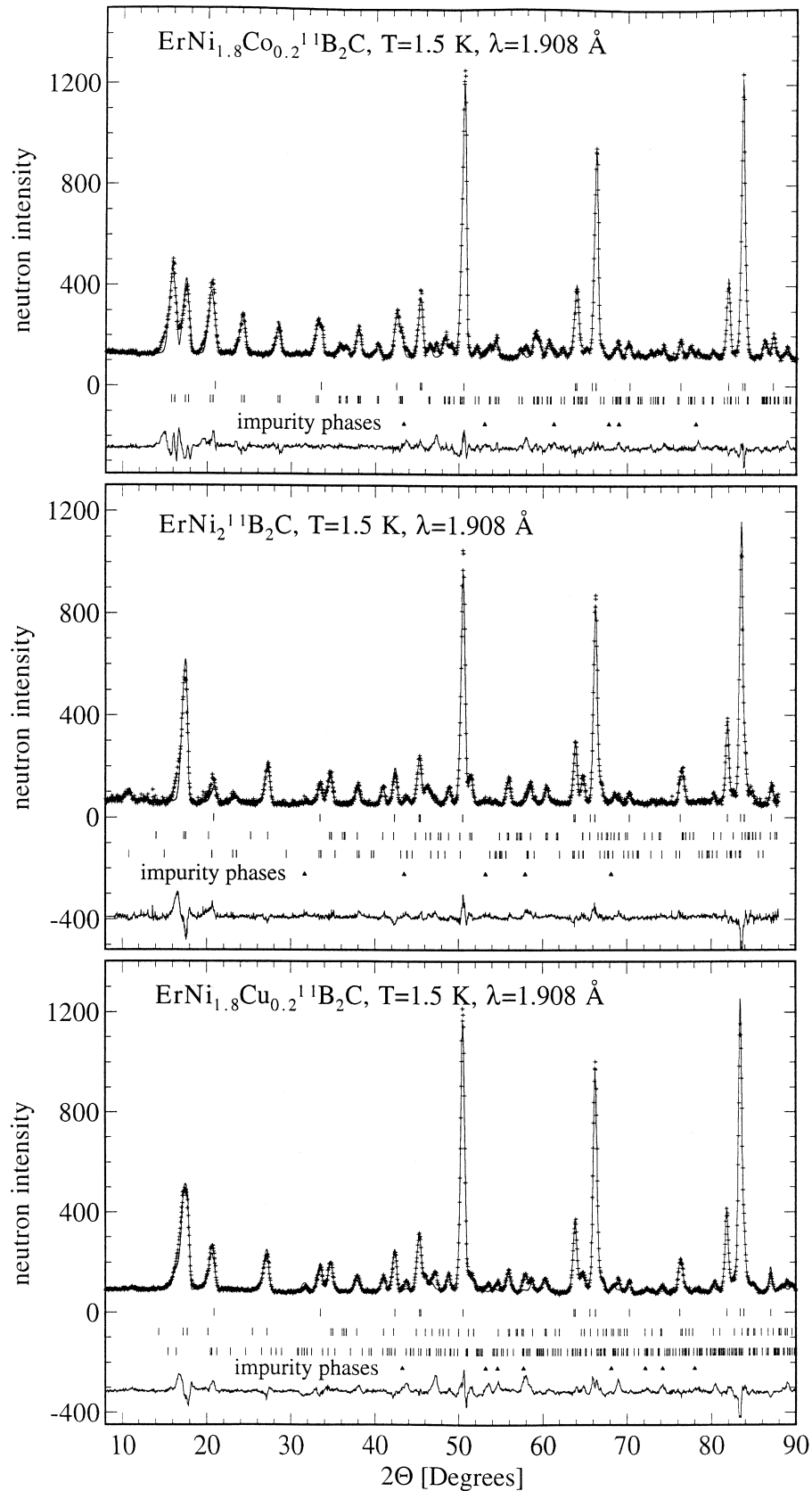


Fig. 6. Neutron diffraction pattern of $\text{ErNi}_{1.8}\text{Co}_{0.2}\text{B}_2\text{C}$, $\text{ErNi}_2\text{B}_2\text{C}$ and $\text{ErNi}_{1.8}\text{Cu}_{0.2}\text{B}_2\text{C}$ in the magnetically ordered state. The position of the magnetic Bragg peaks are given by the 2nd row of vertical ticks.

sample dependent property of $\text{HoNi}_2\text{B}_2\text{C}$ is the occurrence of a third magnetic order: an a -axis incommensurate phase that exists in a limited temperature range above T_N has been observed in some samples [26]. The ordering vector is similar to the one in $\text{ErNi}_2\text{B}_2\text{C}$, but the intensity of the corresponding Bragg peaks is always much smaller than those of the other two phases.

4.2. $\text{ErNi}_2\text{B}_2\text{C}$

In $\text{ErNi}_2\text{B}_2\text{C}$ one magnetic phase transition at $T_m \sim 6$ K has been observed, and the magnetic order co-exists with superconductivity ($T_c = 11$ K) down to the lowest temperatures that were accessible in the experiment (1.5 K). The magnetic moments order in a transversally polarized spin density wave, which is described by the incommensurate ordering vector $k = (0.55, 0, 0)$ (r.l.u.) [or equivalently by $k = (0, 0.55, 0)$ since the lattice is tetragonal]. The moments are aligned parallel to an easy axis and perpendicular to k . At temperatures as low as 1.5 K the observation of reflections belonging to the higher harmonic $3 \cdot k$ shows that the spin density wave is squaring up (Fig. 5). This kind of deviation from the purely sinusoidal order is expected, since a purely sinusoidal spin density wave leaves many spins in a partially unordered state, which cannot be the ground state of the spin system [27]. $\text{RNi}_2\text{B}_2\text{C}$ with $R = \text{Gd, Tb, Ho}$ and Er show incommensurate magnetic orders that are described by k -vectors with k_x or k_y near 0.55 (r.l.u.). This correspondence is due to a maximum in the static susceptibility $\chi(q)$ at $q \sim 0.55$ (r.l.u.) which is a common feature of the $\text{RNi}_2\text{B}_2\text{C}$ compounds. This has been found by calculations of the band structure and the generalized susceptibility [28]. These theoretical considerations show that the maximum in $\chi(q)$ at $q = 0.55$ (r.l.u.) arises from strong Fermi surface nesting. A way to test predictions from calculations of the electronic structure is to vary the Fermi level, E_F . In $\text{RNi}_2\text{B}_2\text{C}$ this can be done in an effective way by doping with Cu and/or Co at the Ni-site since the Ni-3d states make the biggest contribution to the bands near E_F . Indeed neutron diffraction experiments have shown that the magnetic order in $\text{ErNi}_2\text{B}_2\text{C}$ is changing drastically if 10% of Ni is replaced by Co (Fig. 6). This is clear evidence for the strong dependence of the RKKY interaction from the details of the electronic structure, and it confirms the role of Fermi surface nesting in some $\text{RNi}_2\text{B}_2\text{C}$ compounds. In Eq. (4) the dependence of the RKKY interaction on electronic structure is not apparent since in the case of free electrons only the density of states at the Fermi level [$\tilde{N}(E_F)$] enters the expression for $J(R)$.

5. Conclusions

We have presented above a phenomenological approach to the magnetic heat capacity data available for some of

the R123 compounds. The model includes dipolar and exchange interactions. At high oxygen contents all samples which order magnetically do this in a long-range fashion. Oxygen reduction leads in all these compounds to an increase of the anisotropy of the in-plane magnetic coupling due to the competition between the superexchange and the RKKY interaction and – for a restricted oxygen regime – to strong disorder in the electronic and magnetic sublattice. Finally, at low oxygen contents long-range magnetic ordering is recovered due to the reappearance of structural and electronic order in the totally reduced samples. Still unclear is the fact that at high oxygen contents the ordering temperature is very low (for RKKY) and the pressure dependence of the magnetic ordering temperature very strong [29]; more like superexchange than RKKY interaction. This might originate from an almost complete condensation of the holes into Cooper pairs and a resulting inhibition of the polarization of the charge carriers.

The borocarbides are another example for the coexistence of bulk superconductivity with long range magnetic order. But in contrast to the R123 compounds the critical temperatures of magnetic ordering are not reduced compared to non-superconducting $\text{RNi}_2\text{B}_2\text{C}$ compounds ($R = \text{Pr, Nd, Gd}$ and Tb). In this case the simultaneous Cooper pairing and the polarization of the conduction electrons by the rare earth ions cannot be explained by the classical BCS-theory. The richness of magnetic structures is due to the competition of CEF with the RKKY interaction. Furthermore, in $\text{HoNi}_2\text{B}_2\text{C}$ and $\text{ErNi}_2\text{B}_2\text{C}$ the complicated dependence of the RKKY interaction on the details of the electronic structure becomes apparent.

References

- [1] P. Allenspach, B.W. Lee, D.A. Gajewski, M.B. Maple, J. Appl. Phys. 73 (1993) 6317.
- [2] P.C. Canfield, P.L. Gammel, D.J. Bishop, Physics Today (1998) 40, Oct.
- [3] M. Guillaume, U. Staub, F. Fauth, J. Mesot, A. Furrer, C. Carlile, Physica C223 (1994) 333.
- [4] J. Jensen, A.R. Macintosh, Rare Earth Magnetism, Clarendon Press, Oxford, 1991.
- [5] P. Fischer, in: F. Lévy (Ed.), Neutron Scattering in Layered Copper-Oxide Superconductors, Physics and Chemistry of Materials with Low-Dimensional Structures, Kluwer Academic Publishers, The Netherlands, 1998, For an overview of neutron data.
- [6] P. Allenspach, M.B. Maple, Handbook on the Physics and Chemistry of Rare Earths, Vol. 22, in: K.A. Gschneidner, L. Eyring, M.B. Maple (Eds.) In press. For an overview of specific heat data.
- [7] M.B. Maple, J.M. Ferreira, R.R. Hake, B.W. Lee, J.J. Neumeier, C.L. Seaman, K.N. Yang, H. Zhou, J. Less-Comm. Met. 149 (1989) 405.
- [8] B.W. Lee, J.M. Ferreira, Y. Dalichaouch, M.S. Torikachvili, K.N. Yang, M.B. Maple, Phys. Rev. B 37 (4) (1988) 2368.
- [9] P. Allenspach, F. Hulliger, A. Furrer, Phys. Rev. B 39 (1989) 2226.
- [10] P. Allenspach, J. Mesot, U. Staub, M. Guillaume, A. Furrer, S.-I. Yoo, M.J. Kramer, R.W. McCallum, H. Maletta, H. Blank, H.

- Mutka, R. Osborn, M. Arai, Z. Bowden, A.D. Taylor, *Z. Phys. B* 95 (1994) 301.
- [11] M. Guillaume, W. Henggeler, A. Furrer, R.S. Eccleston, V. Trunov, *Phys. Rev. Lett.* 74 (1995) 3423.
- [12] J. Mesot, P. Allenspach, U. Staub, A. Furrer, H. Mutka, R. Osborn, A. Taylor, *Phys. Rev. B* 47 (1993) 6027.
- [13] U. Staub, L. Soderholm, *Handbook on the Physics and Chemistry of Rare Earths*, Vol. 22, K.A. Gschneidner, L. Eyring, M.B. Maple (Eds.). In press.
- [14] A.B. MacIsaac, J.P. Whitehead, K. De'Bell, K. Sowmya Narayanan, *Phys. Rev. B* 46 (10) (1992) 6387.
- [15] P. Fischer, B. Schmid, P. Brüesch, F. Stucki, P. Unternährer, *Z. Phys. B* 74 (1989) 183.
- [16] S. Uma, W. Schnelle, E. Gmelin, G. Rangarajan, A. Erb, E. Walker, R. Flükiger, *Czech. J. Phys.* 46 (Suppl. S5) (1996) 2677.
- [17] M. Buchgeister, W. Hiller, S.M. Hosseini, K. Kopitzki, D. Wagoner, in: R. Niclosky (Ed.), *Proceeding of the International Conference on Transport Properties of Superconductors*, Rio de Janeiro, Brazil, World Scientific Publishing, Singapore, 1990, p. 511.
- [18] C.E.T. Gonçalves da Silva, L.M. Falicov, *J. Phys. C: Solid State Phys.* 5 (1972) 63.
- [19] J. Mesot, P. Allenspach, U. Staub, A. Furrer, H. Mutka, R. Osborn, A. Taylor, *Phys. Rev. B* 47 (10) (1993) 6027.
- [20] J.W. Lynn et al., *Phys. Rev. B* 55 (1997) 6584.
- [21] J. Rossat-Mignod et al., in: K. Sköld, D.L. Price (Eds.), *Methods of Experimental Physics*, Vol. 23C, Academic, Orlando, 1987, Chapter 19.
- [22] J.Y. Rhee et al., *Phys. Rev. B* 51 (1995) 15 585.
- [23] R. Coehoorn, *Physica C* 228 (1994) 331.
- [24] L.F. Mattheiss, *Phys. Rev. B* 49 (1994) 13 279.
- [25] D.J. Singh, *Solid State Commun.* 98 (1996) 899.
- [26] U. Gasser et al., *Z. Phys. B* 101 (1996) 345.
- [27] U. Gasser et al., *Physica C* 282–C287 (1997) 1327.
- [28] J.W. Lynn et al., *J. Appl. Phys.* 79 (1996) 5857.
- [29] P. Allenspach, B.W. Lee, D.A. Gajewski, V.B. Barbeta, M.B. Maple, G. Nieva, S.-I. Yoo, M.J. Kramer, R.W. McCallum, L. Ben-Dor, *Z. Phys. B* 96 (1995) 455.